

Unifying Language-Action Understanding and Generation for Autonomous Driving

Xinyang Wang^{1,2,*} Qian Liu^{2,*} Wenjie Ding^{2,*} Zhao Yang^{2,†} Wei Li²
Chang Liu² Bailin Li² Kun Zhan² Xianpeng Lang² Wei Chen¹

¹State Key Lab of CAD&CG, Zhejiang University ²Li Auto

Abstract

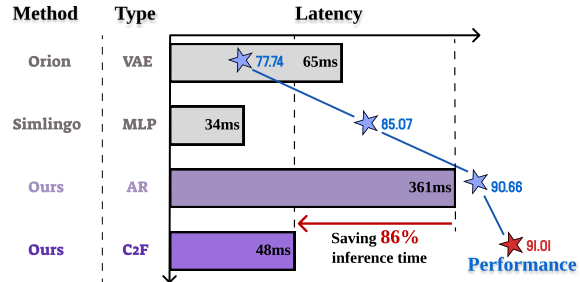
Vision-Language-Action (VLA) models are emerging as a promising paradigm for end-to-end autonomous driving, valued for their potential to leverage world knowledge and reason about complex driving scenes. However, existing methods suffer from two critical limitations: a persistent misalignment between language instructions and action outputs, and the inherent inefficiency of typical autoregressive action generation. In this paper, we introduce **LinkVLA**, a novel architecture that directly addresses these challenges to enhance both alignment and efficiency. First, we establish a structural link by unifying language and action tokens into a shared discrete codebook, processed within a single multi-modal model. This structurally enforces cross-modal consistency from the ground up. Second, to create a deep semantic link, we introduce an auxiliary action understanding objective that trains the model to generate descriptive captions from trajectories, fostering a bidirectional language-action mapping. Finally, we replace the slow, step-by-step generation with a two-step coarse-to-fine generation method (C²F) that efficiently decodes the action sequence, saving 86% inference time. Experiments on closed-loop driving benchmarks show consistent gains in instruction following accuracy and driving performance, alongside reduced inference latency.

1. Introduction

End-to-end learning [3, 5, 13, 14, 22, 30, 31, 42, 51, 55, 60, 61] emerged as a dominant paradigm for developing autonomous driving systems, learning direct sensorimotor policies from raw sensor inputs to vehicle planning. While conventional end-to-end models excel at reactive control in familiar scenarios, they often struggle with complex reasoning, long-tail events, and human interaction [41, 46]. Vision-language-models (VLMs) [11, 16]

Work done while interning at Li Auto.

* Equal contribution. † Project Lead.



(a) Time vs. performance.



(b) Visualization of instruction-following capability.

Figure 1. LinkVLA achieves both higher performance and lower latency in closed-loop evaluation and equipped with superior instruction-following capability.

have attracted significant attention in recent years due to their capable of leveraging extensive world knowledge and sophisticated reasoning capabilities and have been introduced into driving scenarios to enhance their generalization [2, 6, 23–25, 27, 32–35, 45, 49, 50, 52]. Vision-Language-Action (VLA) methods extend VLMs to action generation and have been explored in robotics [1, 36] and autonomous driving [8, 21, 28, 29, 37, 38, 44, 56, 58, 63, 64] to generate physical feasible action based on visual and language inputs. VLAs promise a paradigm shift from learning implicit, reactive policies to developing agents capable of explicit reasoning and long-horizon planning. These models unlock superior interactivity and flexible instruction following, allowing language to serve as a powerful medium for conveying explicit rules and compositional logic, representing a critical step towards achieving more generalist and trustworthy autonomous agents.

At the heart of the VLA paradigm lies the ability to follow natural language instructions. Instruction following is a critical function for real-world deployment, enabling dynamic re-tasking and enhanced user trust through transparent interaction. However, a fundamental challenge plagues current VLA models: a persistent misalignment between language understanding and physical action [10, 37, 49]. A model might correctly generate the decision *change lane to the left*, yet output a lane keep trajectory. This failure in instruction following undermines the core promise of VLAs and poses a significant barrier to their safety and reliability.

Several lines of research have emerged to address the misalignment problem. Some approaches focus on improving data collection techniques [10, 37, 49], a strategy that sidesteps the fundamental modeling challenge. Others rely on post-hoc policy refinement using reinforcement learning [64], which treats alignment as a corrective afterthought. A third vein attempts to align modalities through implicit distribution matching in latent space [8], which lacks a direct, verifiable supervision. In contrast to these methods, we argue that this semantic gap necessitates an explicit bidirectional link woven into the primary supervised learning phase. To this end, we introduce *LinkVLA*, a novel VLA model designed specifically to strengthen this connection.

First, we establish a structural link at the architectural level. By unifying language instructions and trajectories into a shared discrete codebook, we eliminate the modality gap by design, forcing both concepts into a common representational ground. Second, it forges a deep semantic link through a novel bidirectional learning objective. We introduce an explicit action-understanding objective that compels the model to translate the planned actions back into descriptive text. This synergy enforces bidirectional consistency, ensuring the link between language and action is formative and verifiable. While this tightly coupled representation is powerful for alignment, its auto-regressive nature creates an inference bottleneck. To make our framework practical, we replace conventional step-by-step decoding with a coarse-to-fine, two-step generation process. This mechanism first generates a high-level structural outline of the trajectory and then refines this outline into the full, fine-grained path. As visualized in Figure 1, *LinkVLA* not only achieves a dramatic reduction in inference latency but also achieves consistent gains in instruction following accuracy and driving performance. Here are the main contributions:

- A *unified tokenized framework* that learns a shared codebook for language and action, structurally bridging the modality gap to enhance alignment.
- An *explicit action understanding objective* that enforces bidirectional semantic consistency.
- A *coarse-to-fine action generation schema* that drastically reduces inference latency.
- *State-of-the-art performance* on challenging closed-loop

driving benchmarks, demonstrating significant gains in both instruction-following accuracy and driving ability.

2. Related Work

2.1. End-to-end Autonomous Driving

End-to-end autonomous driving has achieved tremendous success in recent years. UniAD [14] adopts an ultimately planning-oriented design philosophy that integrates perception, prediction, and planning into a single network. VAD [22] models driving scenarios into fully vectorized representations, thereby eliminating computationally intensive rasterized representations and resulting in a much faster running speed. ParaDrive [51] proposes a fully parallel end-to-end architecture and conducts a comprehensive exploration of the design space of modular stacks. VADv2 [3] discretizes the planning action space into a large planning vocabulary and leverages extensive driving demonstrations to learn the probability distribution of planning actions. SparseDrive [42] unifies multiple tasks through sparse instance representation and proposes a symmetric sparse perception module and a parallel motion planner. GenAD [61] casts autonomous driving into a generative modeling problem. DriveTransformer [20] adopts task parallelism and sparse representation to improve efficiency by working in a streaming manner. DiffusionDrive [31] uses anchor to truncate the diffusion process, achieving better performance, higher inference efficiency. GoalFlow [55] constrains the generated trajectories by introducing a goal point and use it as the condition of flow matching to generate multimodal trajectories. While proficient at reactive control within known operational domains, these methods display critical limitations in complex logical reasoning, long-tail event processing, and human-interactive task execution.

2.2. VLM and VLA for Autonomous Driving

Early-stage VLMs primarily follow a language-centric paradigm that use visual question answering to describe the action [25, 34, 35]. DriveGPT4 [56] employs Large Language Models (LLMs) to generate scene explanations and control signals. DriveVLM [46] uses VLM to enhance scene understanding and planning capabilities. Drivemlm [50] standardizes decision states to bridge the gap between the language decisions and the vehicle control signals and uses LLM to make driving decisions and explanations. EMMA [15] capitalizes on Gemini’s multimodal capabilities by representing all non-sensor data – including navigation instructions, vehicle status, trajectories, and 3D positions – as textual sequences, thereby transferring pre-trained LLMs’ world knowledge to autonomous driving tasks.

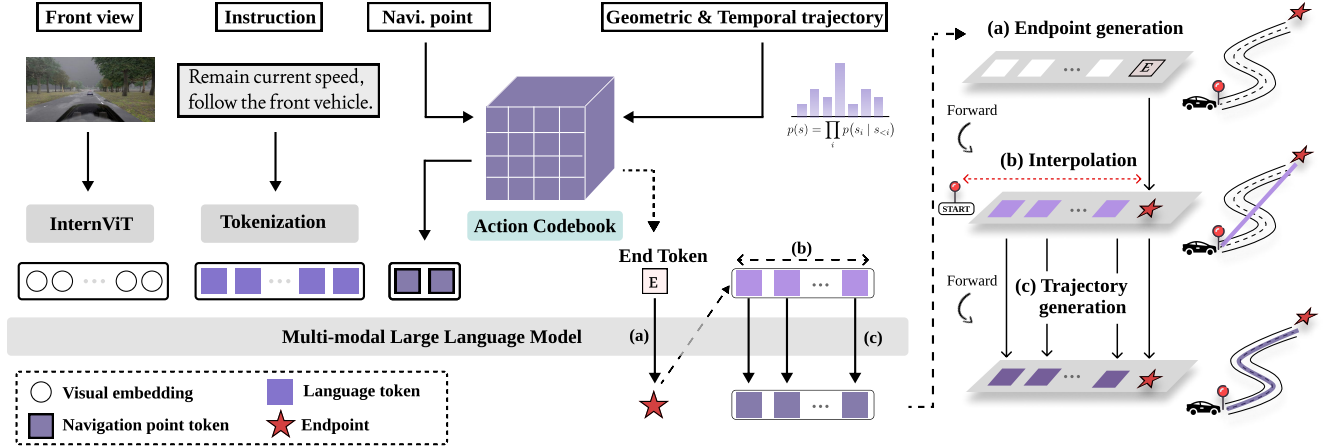


Figure 2. **An overview of the *LinkVLA* architecture.** The model comprises a pretrained InternViT [4] visual backbone and a Qwen2-0.5B [43] LLM. At its core, *LinkVLA* unifies language tokens and action tokens (for navigation points and trajectories) into a single, shared codebook. Training is driven by a unified objective for both language-action understanding and generation, ensuring deep semantic alignment. Inference employs an efficient coarse-to-fine process: first, (a) the model predicts the trajectory endpoint, which is then (b) interpolated into coarse waypoints before being (c) refined into the final, smooth trajectory.

VLA direct outputs action from raw input. Open-drivevla [63] projects visual tokens into a unified semantic space to bridge the modality gap. DriveMoE [57] introduces vision MoE and action MoE to handle diverse scenarios. Recogdrive [29] injects the VLM’s learned driving priors into a diffusion planner and uses reinforcement learning to bridge the gap between language and action. DiffVLA [21] proposes a hybrid sparse-dense diffusion policy empowered by a Vision-Language Model (VLM), enabling efficient multimodal driving behavior generation. However, a modality gap still exists, resulting in misalignment between language and action.

2.3. Language and Action Alignment

AutoVLA [64] unifies reasoning with action generation and employs GRPO [39] to improve planning performance. The step-by-step autoregressive action generation in AutoVLA makes it inefficient in practical deployment. ORION [8] bridges reasoning and action spaces by merging generative planners with VLM architectures, jointly optimizing VQA and planning. SimLingo [37] focuses on aligning linguistic comprehension with driving actions. However, a persistent misalignment between language instructions and action still exist in ORION and SimLingo due to the modal gap. CAST [10] leverage vision language models to create counterfactual labels to augment existing robot datasets. OmniDrive [49] proposes a holistic vision-language dataset for aligning agent models with 3D driving tasks using counterfactual reasoning. In unified multimodal understanding and generation model, understanding and generation are found to be mutually beneficial to each other [47, 54, 62]. Inspired by this, we propose a novel architecture that improves ac-

tion generation ability by introducing an action understanding objective without the need for additional data curation.

3. Method

Our proposed model, *LinkVLA*, is a Vision-Language-Action model designed to enhance language-action alignment and inference efficiency in autonomous driving. Our methodology introduces three key innovations, as illustrated in Figure 2. First, we establish a unified autoregressive framework that models language and action tokens within a single discrete space (Sec. 3.1). Second, to enhance semantic alignment, we introduce a novel action understanding objective that fosters a bidirectional mapping between language and trajectories (Sec. 3.2). Third, we replace slow, sequential decoding with an efficient, coarse-to-fine generation mechanism that drastically reduces inference latency (Sec. 3.3).

3.1. Unified Tokenization Framework

We posit that the language-action misalignment in autonomous driving is a direct consequence of an architectural schism between modalities. To eliminate this, our method is founded on the principle of unification: modeling the entire process—from understanding an instruction to generating a trajectory—within a single unified framework. Our approach maps both the language instruction L and the action trajectory \mathcal{T} into a unified sequence of discrete tokens, which is then processed by a VLM backbone. For language, we leverage the VLM’s existing tokenizer. For actions, which are inherently continuous, we devise a spatial-aware action tokenization scheme. Instead of regressing continuous values, our model predicts a sequence of action tokens

from a tokenized codebook.

Unified Token Space. Our approach is founded on a unified token space for language and action. We achieve this by first quantizing continuous trajectories: the local Bird’s-Eye-View (BEV) space is partitioned into a grid of K_{action} cells, each defining a unique action token. A trajectory $\mathcal{T} = \{w_1, \dots, w_T\}$ is thus converted into a sequence of action tokens $A = \{a_1, \dots, a_T\}$ by mapping each waypoint to its corresponding cell. This action codebook (\mathcal{C}_{action}) is then merged with the model’s text vocabulary (size K_{text}) to form a single, unified codebook \mathcal{C} of size $K = K_{text} + K_{action}$. The action token embeddings are learned end-to-end, forcing the model to map linguistic and spatial concepts into a shared representation and enabling a single VLM model to process both. During inference, each predicted action token is simply decoded back to the center of its corresponding grid cell.

Action Tokenization. Naive tokenization, which tokenizes waypoints onto a uniform BEV grid using one-hot labels, suffers from two key issues. First, a uniform grid allocates resolution evenly, failing to provide the fine-grained precision essential for near-field control. Second, the hard assignment of one-hot labels discards the grid’s inherent spatial topology, complicating the learning of spatial priors. To mitigate these issues, we introduce two key refinements: Log Coordinate Transformation and Spatial Soft-labeling.

1) *Log Coordinate Transformation.* We devise a non-uniform quantization scheme that prioritizes precision near the ego-vehicle. This is achieved by first applying a non-linear transformation to the waypoint coordinates (x, y) independently along each axis. Specifically, each coordinate $z \in \{x, y\}$ is transformed using a signed logarithmic function:

$$z' = \text{sign}(z) \cdot \log(1 + k \cdot |z|). \quad (1)$$

Here, k is a positive scaling factor that controls the size of the linear region around the origin. The resulting transformed space (x', y') is then uniformly quantized to produce the action tokens.

2) *Spatial Soft-labeling.* To embed a physical prior about the continuity of the action space into our learning objective, we employ a spatial soft-labeling strategy. A standard one-hot target provides a discrete supervisory signal, but does not explicitly account for the spatial topology of our action grid. Our approach refines this by defining a smooth target distribution that acknowledges spatial adjacency.

Specifically, for a ground-truth token a_{gt} , we construct the target distribution $q(a)$ over all action tokens $a \in \mathcal{C}_{action}$ as a normalized 2D Gaussian centered on the co-

ordinates of a_{gt} with radius R :

$$q(a) = \frac{1}{Z} \exp\left(-\frac{\|\text{pos}(a) - \text{pos}(a_{gt})\|_2^2}{2\sigma^2}\right), \quad (2)$$

where $\text{pos}(a)$ maps an action token to its 2D coordinates in the spatial grid, $\|\cdot\|_2^2$ is the squared Euclidean distance, σ is a hyperparameter controlling the spread of the distribution, and Z is a normalization constant ensuring $\sum_{a \in \mathcal{C}_{action}} q(a) = 1$. For action generation, the model’s predicted distribution $p(a)$ is then optimized to match this soft target using the cross-entropy loss:

$$\mathcal{L}_{\text{generation}} = - \sum_{a \in \mathcal{C}_{action}} q(a) \log p(a). \quad (3)$$

This objective encourages the model to assign probability mass not only to the correct token but also to its spatial neighbors, as dictated by the Gaussian shape. This fosters a locally smooth action manifold, making the model more robust to minor groundtruth errors. When incorporating chain-of-thought, an additional standard cross-entropy loss for language generation is added to this objective.

3.2. Unified Language-Action Understanding and Generation

To strengthen the link between language and behavior, we introduce a bidirectional training objective inspired by the duality of image captioning and text-to-image generation. In generative vision-language modeling, the tasks of generating text L from an image V ($p(L|V)$) and an image from text ($p(V|L)$) are reciprocal [47, 54, 62]. Training a model on both objectives has been shown to produce a more robust and aligned joint embedding space.

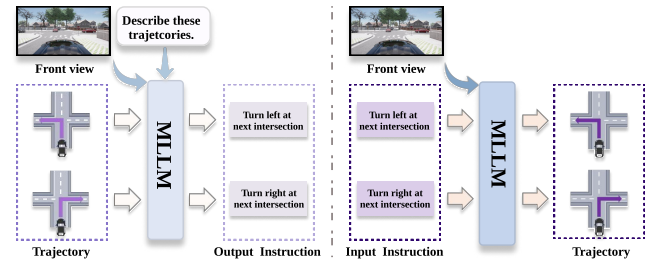


Figure 3. Illustration of the action understanding (Left) and the action generation (Right).

We posit that a similar duality exists for the language-action mapping within VLA models. The conventional task is *action generation*, where a language instruction guides the prediction of an action sequence A ($p(A|L)$). This is analogous to text-to-image synthesis. We propose its reciprocal: *action understanding*, where an executed action sequence A is used to infer the original language instruction ($p(L|A)$). This mirrors image captioning, as the

model must produce a linguistic description explaining the observed behavior. Crucially, both of these mappings are grounded in a shared visual context V , which provides the necessary environmental awareness. Formally, besides $\mathcal{L}_{generation}$ (Eq. 3), we introduce a reciprocal objective designed for reconstructing the language instruction L given the vision and action inputs:

$$\mathcal{L}_{understanding} = - \sum_j \log p(l_j | V, A, l_{<j}), \quad (4)$$

where $l_{<j}$ represents the preceding ground-truth tokens.

The final training objective is a weighted sum of these two losses: $\mathcal{L}_{total} = \mathcal{L}_{generation} + \lambda \mathcal{L}_{understanding}$, where λ is a balancing hyperparameter. By forcing the model to solve this inverse problem, we enforce a bidirectional consistency within the shared embedding space. This process enriches the semantic grounding of the action tokens, ensuring they are intrinsically linked to descriptive linguistic concepts, thereby leading to better instruction following. In practice, both tasks are handled by the same decoder by simply swapping the roles of L and A as the prediction target.

3.3. Coarse-to-Fine Action Generation

Auto-regressive generation of a long trajectory of T waypoints requires T sequential forward passes, which is computationally expensive and introduces significant inference latency. To address this, we collapse the T -step sequential dependency into a two-stage process: (1) endpoint prediction and coarse trajectory initialization, and (2) parallel trajectory refinement. Following [37], our action outputs include both temporal speed waypoints and geometric path waypoints. As both are treated as point sequences and processed symmetrically throughout our framework, we will hereafter refer to them collectively as a *trajectory* and its constituents as *waypoints* for clarity.

Training with a Coarse Trajectory Prior. Our coarse-to-fine inference is enabled by a carefully designed training objective. To directly predict endpoints, we put special tokens at the beginning of the decoder’s input sequence. During training, the ground-truth target sequence is reordered, $\{w_T, w_1, w_2, \dots, w_{T-1}\}$, teaching the model to associate the special token with the endpoint prediction. For the refinement stage, we simulate coarse trajectory via linear interpolation using the groundtruth endpoint, quantize it into coarse waypoint tokens as model inputs, and train the model to map these coarse tokens to the corresponding fine-grained trajectory.

Coarse Trajectory Initialization. During inference, we first establish a strong structural prior for the trajectory, which serves to guide the subsequent generation steps. With

our modified training sequence, the model performs a single forward pass to predict specifically the final waypoint, \hat{w}_T . While this initial step is inspired by goal-point prediction methods [55], our approach is fundamentally distinct as we integrate endpoint prediction and trajectory refinement within a single, unified transformer architecture.

Given the start point w_0 (the ego-vehicle’s origin at $(0, 0)$) and the predicted end point w_T , we construct the coarse trajectory, \mathcal{W}_{coarse} , via linear interpolation:

$$w_i^{coarse} = w_0 + \frac{i}{T}(w_T - w_0) \quad \text{for } i \in \{1, \dots, T\} \quad (5)$$

Then these waypoints are tokenized into trajectory tokens, as an initial scaffold for the subsequent refinement stage.

Parallel Trajectory Refinement. The second inference step refines the coarse, straight-line path into a dynamically feasible trajectory. We formulate this as a structure-preserving refinement, where each coarse waypoint w_i^{coarse} is mapped to its corresponding refined waypoint w_i^{fine} . Given tokenized coarse waypoints as initial input, LinkVLA predicts T refined points in parallel. Conditioned by the vision-language context via cross-attention, the refined path respects lane boundaries, avoids obstacles, and adheres to the language instruction.

4. Experiments

We first introduce the benchmarks, evaluation metrics (Sec. 4.1), and implementation details (Sec. 4.2). Then we present and analyze the closed-loop results and the instruction-following ability (Sec. 4.3), followed by detailed ablation experiment and comparisons (Sec. 4.4).

4.1. Settings

Bench2Drive. We train and evaluate LinkVLA using the Bench2Drive benchmark [19], which provides a set of interactive scenarios within the widely used CARLA simulator [7]. We follow SimLingo [37] and use an open-source expert PDM-lite [41] to collect driving dataset in the CARLA simulator. Our evaluation follows the CARLA v2 closed-loop protocol for end-to-end autonomous driving, comprising 44 interactive scenarios with 5 routes each, for a total of 220 official routes across diverse weather conditions. We report performance using the benchmark’s official metrics: Driving Score (DS), Success Rate (SR), Efficiency, Comfortness, and Multi-Ability.

Instruction-following Evaluation. We evaluate the model’s instruction-following capabilities using the *Action Dreaming* dataset from SimLingo [37]. This dataset is designed to assess a model’s ability not only to comprehend scene-specific knowledge from language but also to translate this understanding into the corresponding action space.

Table 1. **Main results and multi-ability in Bench2Drive.** * denote expert feature distillation.

Method	Closed-loop metrics \uparrow				Multi-Ability (%) \uparrow					
	DS	SR (%)	Efficiency	Comfort.	Merging	Overtake	Brake	Give-Way	Traffic-Sign	Mean
TCP* [53]	40.70	15.00	54.26	47.80	16.18	20.00	20.00	10.00	6.99	14.63
TCP-ctrl*	30.47	7.27	55.97	51.51	10.29	4.44	10.00	10.00	6.45	8.23
TCP-traj*	59.90	30.00	76.54	18.08	8.89	24.29	51.67	40.00	46.28	34.22
ThinkTwice* [18]	62.44	31.23	69.33	16.22	27.38	18.42	35.82	50.00	54.23	37.17
DriveAdapter* [17]	64.22	33.08	70.22	16.01	28.82	26.38	48.76	50.00	56.43	42.08
AD-MLP [59]	18.05	0.00	48.45	22.63	0.00	0.00	0.00	0.00	4.35	0.87
UniAD-Tiny [14]	40.73	13.18	123.92	47.04	8.89	9.33	20.00	20.00	15.43	14.73
UniAD-Base [14]	45.81	16.36	129.21	43.58	14.10	17.78	21.67	10.00	14.21	15.55
VAD [22]	42.35	15.00	157.94	46.01	8.11	24.44	18.64	20.00	19.15	18.07
DriveTransformer [20]	63.46	35.01	100.64	20.78	17.57	35.00	48.36	40.00	52.10	38.60
Orion [8]	77.74	54.62	151.48	17.38	25.00	71.11	78.33	30.00	69.15	54.72
AutoVLA [64]	78.84	57.73	146.93	39.33	-	-	-	-	-	-
SimLingo [37]	85.07	67.27	259.23	33.67	53.75	68.89	81.67	50.00	82.11	67.28
LinkVLA (Ours)	91.01	74.55	255.84	34.62	60.00	80.00	93.33	50.00	83.68	73.40

Given a natural language instruction, the model is expected to generate a sequence of actions that corresponds to the command. The evaluation is conducted on the CARLA Town 13 dreamer dataset for validation. The instructions belong to one of six classes: Slow down, Speed up, Reach target speed, Lane change, Object centric. Performance is measured by the success rate.

DriveLM-hard (VQA) and Commentary. We evaluate VQA and commentary generation on the DriveLM-hard benchmark [37]. This challenging validation set is derived from DriveLM [41] and focuses on the CARLA Town 13 environment. To ensure a balanced test that includes rare cases, the benchmark was constructed by uniformly sampling 10 examples per answer type, rather than using simple random sampling. The final dataset contains 330 VQA answer types and 190 Commentary types. We report scores using the *SPICE*, *BLEU*, and *ROUGE-L* metrics.

Table 2. **Performance and Latency Comparison.** All metrics are evaluated on the CARLA benchmark. Latency is the average inference time per step, measured on H20 GPU.

ID	Method	Type	Latency \downarrow	Driving Score \uparrow
1	Orion [8]	VAE	65ms	77.74
2	Simlingo [37]	MLP	34ms	85.07
3	Ours	AR	361ms	90.66
4	Ours	C2F	48ms	91.01

4.2. Implementation details

Action Tokenize. The framework operates within a Bird’s-Eye-View (BEV) space spanning the coordinate ranges $x \in [0, 50]$ m and $y \in [-30, 30]$ m. To create a discrete action space, these coordinates are first transformed using the logarithmic function detailed in Sec 3.1 (with hyperparameter $k = 5$) and subsequently discretized into a uniform grid with a 0.1 step size. This process yields a 56×101 grid, which constitutes a vocabulary of $K_{action} = 5,656$ discrete action tokens. For the spatial soft-labeling procedure, a neighbor weighting radius of $R = 10$ cells and a Gaussian standard deviation of $\sigma = 1.2$ are employed. Furthermore, to enable hierarchical action generation for the coarse-to-fine (C2F) framework, two special tokens are introduced: the *path goal token* and the *waypoint goal token*.

Training Details. We use the InternVL2-1B from the Mini-InternVL family [9] as our main architecture. The InternVL2-1B [9] model consists of the vision encoder InternViT-300M-448px (ViT) [4] and Qwen2-0.5B-Instruct [43] as the language model (LLM). We train our model using the AdamW optimizer [26] with a cosine learning rate schedule. The hyperparameters are set as follows: a base learning rate of 1e-4, weight decay of 0.1, $\beta_1 = 0.9$, $\beta_2 = 0.999$, and a dropout rate of 0.1. The model is trained for 30 epochs on 32 H20 GPUs with a batch size of 48. For model adaptation, we follow SimLingo [37] and apply LoRA [12] with a rank of 32 and $\alpha = 64$.

During inference, we employ a Chain-of-Thought (CoT) approach. First, the model generates a textual rationale for the action. Conditioned on this commentary, it then pre-

dicts the final action sequence. This output consists of 20 geometric path tokens and 10 temporal waypoint tokens per frame.

Unified understanding and generation. We randomly concatenate a (V, L, A) tuple to: 1) $[V, A, L]$ and supervise L for action understanding, or 2) $[V, L, A]$ and supervise A for action generation. Both are trained together with \mathcal{L}_{total} .

4.3. Results

Bench2Drive Results. Table 1 reports closed-loop metrics and multi-ability evaluations on Bench2Drive. LinkVLA archives the highest driving score and success rate while maintaining comparable efficiency and comfortness. Concretely, LinkVLA achieves driving score of 91.01 and an success rate of 74.55, surpassing the previous state of the art, SimLingo (85.07 DS, 67.27 SR), by 5.94 and 7.28 points, respectively, corresponding to relative gains of 6.98% and 10.82%. For efficiency, LinkVLA reaches 255.84, markedly exceeding earlier methods such as Orion (151.48) and AutoVLA (146.93). For comfortness, LinkVLA (34.62) modestly surpasses SimLingo (33.67) and substantially outperforms Orion (17.38).

The multi-ability results show robust driving behavior across diverse interaction scenarios. LinkVLA achieves the best scores in Merging (60.00), Overtake (80.00), Brake (93.33), and Traffic-Sign (83.68), and matches the top performance on Give-Way (50.00). The gains are especially pronounced in interaction-heavy and hazard-responsive skills, with improvements over SimLingo of 6.25 points in Merging, 11.11 in Overtake, and 11.66 in Brake. The overall multi-ability performance reaches 73.40, outperforming SimLingo (67.28) by 6.12 points (9.09% relative) and Orion (54.72) by 18.68, indicating that LinkVLA is better for closed-loop driving performance.

Inference Latency. Table 2 presents a comparative analysis of the latency-performance on the Bench2Drive benchmark. Latency is quantified as the average inference time to generate one compact trajectory per frame. We omit the computational cost of the Chain-of-Thought (CoT) process, as its variable, query-dependent nature would introduce a confounding factor into the latency analysis.

Among the baselines, SimLingo is the fastest with a latency of 34 ms per step but achieves a Driving Score of 85.07. In contrast, Orion (VAE) is slower at 65 ms. Our auto-regressive (AR) variant achieves a high Driving Score of 90.66 but at a prohibitive latency of 361 ms.

In contrast, our proposed C2F method achieves a superior balance. It reduces latency from 361 ms to 48 ms, while simultaneously increasing the Driving Score to 91.01, the highest among all compared methods, achieving a 13.27-point higher Driving Score with 26% lower latency than Orion. Compared to the fastest baseline, SimLingo, our method provides a 5.94-point performance gain with only a modest 14 ms increase in latency.

4.4. Comparison Analysis

Instruction-following Evaluation. Our instruction-following evaluation, detailed in Table 3, shows that the progressive addition of action tokenization, coarse-to-fine (C2F) trajectory generation, and the action understanding objective for alignment (short for *align.* in table) substantially improves performance. Compared to the baseline (ID 1, 70.11% mean success), introducing tokenization alone (ID 2) boosts the overall success rate to 81.63%. This gain is driven by near-perfect performance on the Stop task (99.88%) and significant improvements in Lane Change (88.49%) and Object centric (84.34%). Subsequently adding C2F generation (ID 3) further enhances performance on tasks such as Faster (93.16%), Target Speed (69.24%), and Lane Change (95.45%). Finally, incorporating the alignment module (ID 4) yields the most optimal and balanced performance. This final configuration achieves the highest mean success rate of 87.16% and sets new peak scores for Faster (96.48%), Target Speed (74.73%), and Lane Change (97.42%), demonstrating the surprising instruction-following ability of our method and the effectiveness of our proposed action understanding objective.

Language Ability Evaluation. Table 4 indicates that across both benchmarks, enabling tokenization (ID 2) yields consistent gains over the baseline (ID 1) in *SPICE*, *BLEU*, and *ROUGE-L*. Adding C2F (ID 3) further strengthens semantic fidelity: *SPICE* rises on both DriveLM-VQA (to 71.3) and commentary (to 53.6). Incorporating alignment training in addition to tokenization and C2F (ID 4) yields the best language understand performance in both VQA and commentary benchmarks, with all metrics improved. Thanks to the unified token space design, our model has achieved more outstanding language ability.

Ablation Experiment. Table 5 shows that tokenization yields the large improvement, increasing the driving score from 85.07% to 89.57% and the success rate from 67.27% to 73.18%. Adding C2F without alignment produces a marginal gain in driving score (to 89.85%) and slightly reduces success rate (to 72.27%). Incorporating alignment in addition to tokenization and C2F yields the best performance (driving score 91.01%; success rate 74.55%), surpassing all prior configurations.

Effect of Soft-labeling. Table S2 shows that adding soft-label supervision yields consistent gains in closed-loop performance. The driving score increases from 90.85 to 91.01 (by 0.16 points), and the success rate rises from 72.73% to 74.55% (by 1.82 points). These results suggest that soft-label supervision effectively leverages spatial prior and results in robust driving performance and task completion.

Navigation Modalities. Table 7 shows that the two navigation modalities deliver comparable closed-loop performance. It shows the ability of the LinkVLA to follow basic

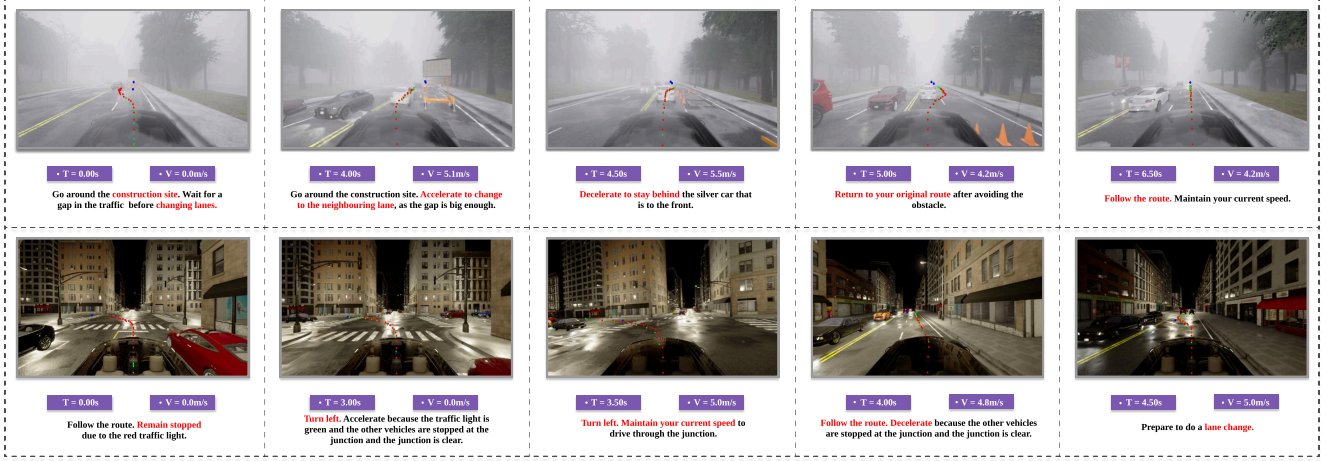


Figure 4. Visualization in challenging environment with various language instructions. The generated trajectory accurately adheres to the language instruction while remaining safe and feasible within the complex environment.

Table 3. **Instruction-following evaluation** on *Action Dreaming* dataset [37]. Align. refers to alignment with unified training.

ID	Token	C2F	Align.	Success Rate (%) \uparrow						
				Faster	Slower	Target Speed	Lane Change	Object	Stop	Mean
1	\times	\times	\times	81.42	61.83	66.27	75.53	74.69	60.93	70.11
2	\checkmark	\times	\times	88.44	65.24	63.37	88.49	84.34	99.88	81.63
3	\checkmark	\checkmark	\times	93.16	55.86	69.24	95.45	85.38	92.14	81.87
4	\checkmark	\checkmark	\checkmark	96.48	65.57	74.73	97.42	91.41	97.34	87.16

Table 4. **Language Ability** in DriveLM-VQA and commentary evaluation. S / B / R refers to *SPICE* / *BLEU* / *ROUGE-L*

ID	Token	C2F	Align.	DriveLM-VQA \uparrow			Commentary \uparrow		
				S	B	R	S	B	R
1	\times	\times	\times	66.7	68.9	71.5	49.2	60.3	64.3
2	\checkmark	\times	\times	69.7	70.5	73.1	53.3	63.7	68.0
3	\checkmark	\checkmark	\times	71.3	69.9	73.4	53.6	61.6	67.3
4	\checkmark	\checkmark	\checkmark	73.0	74.7	77.0	57.4	65.7	70.8

Table 6. Effect of soft label in close-loop evaluation.

Method	Driving Score \uparrow	Success Rate (%) \uparrow
Ours w/o. soft label	90.85	72.73
Ours w/. soft label	91.01	74.55

navigational commands and navigational GPS target points with the same model.

Additional ablation Discussions. Due to space limitation, we further provide more extensive ablation studies on action codebook size K_{action} , scaling factor k in the log transformation, and the spread scale parameter σ in the spatial soft-

Table 5. **Closed-loop performance** ablation study with different components we proposed.

ID	Token	C2F	Align.	Closed-loop metrics \uparrow	
				Driving Score	Success Rate (%)
1	\times	\times	\times	85.07	67.27
2	\checkmark	\times	\times	89.57	73.18
3	\checkmark	\checkmark	\times	89.85	72.27
4	\checkmark	\checkmark	\checkmark	91.01	74.55

Table 7. Effect of different navigation forms.

Method	Driving Score \uparrow	Success Rate (%) \uparrow
GPS target point	91.01	74.55
Navigation command	91.25	73.18

labeling in *Supplementary Materials*.

5. Conclusion

We present *LinkVLA*, a novel VLA model that improves language-action alignment and efficiency. We achieve deep cross-modal consistency by unifying language and

action tokens in a shared codebook and training a novel bidirectional captioning objective. This core strategy, coupled with a coarse-to-fine decoder that cuts latency by 86%, delivers substantial gains in instruction following and driving performance on closed-loop benchmarks. Our work thus provides a practical path toward reliable and responsive language-guided agents for real-world deployment.

References

- [1] Kevin Black, Noah Brown, Danny Driess, Adnan Esmail, Michael Equi, Chelsea Finn, Niccolo Fusai, Lachy Groom, Karol Hausman, Brian Ichter, et al. π 0: A vision-language-action flow model for general robot control. corr, abs/2410.24164, 2024. doi: 10.48550. *arXiv preprint ARXIV.2410.24164*. 1
- [2] Kai Chen, Yanze Li, Wenhua Zhang, Yanxin Liu, Pengxiang Li, Ruiyuan Gao, Lanqing Hong, Meng Tian, Xinhai Zhao, Zhenguang Li, et al. Automated evaluation of large vision-language models on self-driving corner cases. In *2025 IEEE/CVF Winter Conference on Applications of Computer Vision (WACV)*, pages 7817–7826. IEEE, 2025. 1
- [3] Shaoyu Chen, Bo Jiang, Hao Gao, Bencheng Liao, Qing Xu, Qian Zhang, Chang Huang, Wenyu Liu, and Xinggang Wang. Vadv2: End-to-end vectorized autonomous driving via probabilistic planning. *arXiv preprint arXiv:2402.13243*, 2024. 1, 2
- [4] Zhe Chen, Jiannan Wu, Wenhai Wang, Weijie Su, Guo Chen, Sen Xing, Muyan Zhong, Qinglong Zhang, Xizhou Zhu, Lewei Lu, et al. Internvl: Scaling up vision foundation models and aligning for generic visual-linguistic tasks. In *Proceedings of the IEEE/CVF conference on computer vision and pattern recognition*, pages 24185–24198, 2024. 3, 6
- [5] Kashyap Chitta, Aditya Prakash, Bernhard Jaeger, Zehao Yu, Katrin Renz, and Andreas Geiger. Transfuser: Imitation with transformer-based sensor fusion for autonomous driving. *IEEE transactions on pattern analysis and machine intelligence*, 45(11):12878–12895, 2022. 1
- [6] Kairui Ding, Boyuan Chen, Yuchen Su, Huan-ang Gao, Bu Jin, Chonghao Sima, Wuqiang Zhang, Xiaohui Li, Paul Barsch, Hongyang Li, et al. Hint-ad: Holistically aligned interpretability in end-to-end autonomous driving. *arXiv preprint arXiv:2409.06702*, 2024. 1
- [7] Alexey Dosovitskiy, German Ros, Felipe Codevilla, Antonio Lopez, and Vladlen Koltun. Carla: An open urban driving simulator. In *Conference on robot learning*, pages 1–16. PMLR, 2017. 5, 1
- [8] Haoyu Fu, Diankun Zhang, Zongchuang Zhao, Jianfeng Cui, Dingkan Liang, Chong Zhang, Dingyuan Zhang, Hongwei Xie, Bing Wang, and Xiang Bai. Orion: A holistic end-to-end autonomous driving framework by vision-language instructed action generation. In *Proceedings of the IEEE/CVF International Conference on Computer Vision*, 2025. 1, 2, 3, 6
- [9] Zhangwei Gao, Zhe Chen, Erfei Cui, Yiming Ren, Weiyun Wang, Jinguo Zhu, Hao Tian, Shenglong Ye, Junjun He, Xizhou Zhu, et al. Mini-internvl: a flexible-transfer pocket multi-modal model with 5% parameters and 90% performance. *Visual Intelligence*, 2(1):32, 2024. 6
- [10] Catherine Glossop, William Chen, Arjun Bhorkar, Dhruv Shah, and Sergey Levine. Cast: Counterfactual labels improve instruction following in vision-language-action models. *arXiv preprint arXiv:2508.13446*, 2025. 2, 3
- [11] Daya Guo, Dejian Yang, Haowei Zhang, Junxiao Song, Ruoyu Zhang, Runxin Xu, Qihao Zhu, Shirong Ma, Peiyi Wang, Xiao Bi, et al. Deepseek-r1: Incentivizing reasoning capability in llms via reinforcement learning. *arXiv preprint arXiv:2501.12948*, 2025. 1
- [12] Edward J Hu, Yelong Shen, Phillip Wallis, Zeyuan Allen-Zhu, Yuanzhi Li, Shean Wang, Lu Wang, Weizhu Chen, et al. Lora: Low-rank adaptation of large language models. *ICLR*, 1(2):3, 2022. 6
- [13] Shengchao Hu, Li Chen, Penghao Wu, Hongyang Li, Junchi Yan, and Dacheng Tao. St-p3: End-to-end vision-based autonomous driving via spatial-temporal feature learning. In *European Conference on Computer Vision*, pages 533–549. Springer, 2022. 1
- [14] Yihan Hu, Jiazhi Yang, Li Chen, Keyu Li, Chonghao Sima, Xizhou Zhu, Siqi Chai, Senyao Du, Tianwei Lin, Wenhai Wang, et al. Planning-oriented autonomous driving. In *Proceedings of the IEEE/CVF conference on computer vision and pattern recognition*, pages 17853–17862, 2023. 1, 2, 6
- [15] Jyh-Jing Hwang, Runsheng Xu, Hubert Lin, Wei-Chih Hung, Jingwei Ji, Kristy Choi, Di Huang, Tong He, Paul Covington, Benjamin Sapp, et al. Emma: End-to-end multimodal model for autonomous driving. *arXiv preprint arXiv:2410.23262*, 2024. 2
- [16] Aaron Jaech, Adam Kalai, Adam Lerer, Adam Richardson, Ahmed El-Kishky, Aiden Low, Alec Helyar, Aleksander Madry, Alex Beutel, Alex Carney, et al. Openai o1 system card. *arXiv preprint arXiv:2412.16720*, 2024. 1
- [17] Xiaosong Jia, Yulu Gao, Li Chen, Junchi Yan, Patrick Langechuan Liu, and Hongyang Li. Driveadapter: Breaking the coupling barrier of perception and planning in end-to-end autonomous driving. In *Proceedings of the IEEE/CVF International Conference on Computer Vision*, pages 7953–7963, 2023. 6
- [18] Xiaosong Jia, Penghao Wu, Li Chen, Jiangwei Xie, Conghui He, Junchi Yan, and Hongyang Li. Think twice before driving: Towards scalable decoders for end-to-end autonomous driving. In *Proceedings of the IEEE/CVF Conference on Computer Vision and Pattern Recognition*, pages 21983–21994, 2023. 6
- [19] Xiaosong Jia, Zhenjie Yang, Qifeng Li, Zhiyuan Zhang, and Junchi Yan. Bench2drive: Towards multi-ability benchmarking of closed-loop end-to-end autonomous driving. In *NeurIPS 2024 Datasets and Benchmarks Track*, 2024. 5, 1
- [20] Xiaosong Jia, Junqi You, Zhiyuan Zhang, and Junchi Yan. Drivetransformer: Unified transformer for scalable end-to-end autonomous driving. In *International Conference on Learning Representations (ICLR)*, 2025. 2, 6
- [21] Anqing Jiang, Yu Gao, Zhigang Sun, Yiru Wang, Jijun Wang, Jinghao Chai, Qian Cao, Yuweng Heng, Hao Jiang, Yunda Dong, et al. Diffvla: Vision-language guided dif-

- fusion planning for autonomous driving. *arXiv preprint arXiv:2505.19381*, 2025. 1, 3
- [22] Bo Jiang, Shaoyu Chen, Qing Xu, Bencheng Liao, Jiajie Chen, Helong Zhou, Qian Zhang, Wenyu Liu, Chang Huang, and Xinggong Wang. Vad: Vectorized scene representation for efficient autonomous driving. In *Proceedings of the IEEE/CVF International Conference on Computer Vision*, pages 8340–8350, 2023. 1, 2, 6
- [23] Bo Jiang, Shaoyu Chen, Bencheng Liao, Xingyu Zhang, Wei Yin, Qian Zhang, Chang Huang, Wenyu Liu, and Xinggong Wang. Senna: Bridging large vision-language models and end-to-end autonomous driving. *arXiv preprint arXiv:2410.22313*, 2024. 1
- [24] Bo Jiang, Shaoyu Chen, Qian Zhang, Wenyu Liu, and Xinggong Wang. Alphadrive: Unleashing the power of vlms in autonomous driving via reinforcement learning and reasoning. *arXiv preprint arXiv:2503.07608*, 2025.
- [25] Bu Jin and Haotian Liu. Adapt: Action-aware driving caption transformer. In *CAAI International Conference on Artificial Intelligence*, pages 473–477. Springer, 2023. 1, 2
- [26] Diederik Kinga, Jimmy Ba Adam, et al. A method for stochastic optimization. In *International conference on learning representations (ICLR)*. California, 2015. 6
- [27] Boyi Li, Yue Wang, Jiageng Mao, Boris Ivanovic, Sushant Veer, Karen Leung, and Marco Pavone. Driving everywhere with large language model policy adaptation. In *Proceedings of the IEEE/CVF Conference on Computer Vision and Pattern Recognition*, pages 14948–14957, 2024. 1
- [28] Yingyan Li, Shuyao Shang, Weisong Liu, Bing Zhan, Haochen Wang, Yuqi Wang, Yuntao Chen, Xiaoman Wang, Yasong An, Chufeng Tang, et al. Drivevla-w0: World models amplify data scaling law in autonomous driving. *arXiv preprint arXiv:2510.12796*, 2025. 1
- [29] Yongkang Li, Kaixin Xiong, Xiangyu Guo, Fang Li, Sixu Yan, Gangwei Xu, Lijun Zhou, Long Chen, Haiyang Sun, Bing Wang, et al. Recogdrive: A reinforced cognitive framework for end-to-end autonomous driving. *arXiv preprint arXiv:2506.08052*, 2025. 1, 3
- [30] Zhenxin Li, Kailin Li, Shihao Wang, Shiyi Lan, Zhiding Yu, Yishen Ji, Zhiqi Li, Ziyue Zhu, Jan Kautz, Zuxuan Wu, et al. Hydra-mdp: End-to-end multimodal planning with multi-target hydra-distillation. *arXiv preprint arXiv:2406.06978*, 2024. 1
- [31] Bencheng Liao, Shaoyu Chen, Haoran Yin, Bo Jiang, Cheng Wang, Sixu Yan, Xinbang Zhang, Xiangyu Li, Ying Zhang, Qian Zhang, et al. Diffusiondrive: Truncated diffusion model for end-to-end autonomous driving. In *Proceedings of the Computer Vision and Pattern Recognition Conference*, pages 12037–12047, 2025. 1, 2
- [32] Yingzi Ma, Yulong Cao, Jiachen Sun, Marco Pavone, and Chaowei Xiao. Dolphins: Multimodal language model for driving. In *European Conference on Computer Vision*, pages 403–420. Springer, 2024. 1
- [33] Jiageng Mao, Yuxi Qian, Junjie Ye, Hang Zhao, and Yue Wang. Gpt-driver: Learning to drive with gpt. *arXiv preprint arXiv:2310.01415*, 2023.
- [34] Ana-Maria Marcu, Long Chen, Jan Hünemann, Alice Karnsund, Benoit Hanotte, Prajwal Chidananda, Saurabh Nair, Vijay Badrinarayanan, Alex Kendall, Jamie Shotton, et al. Lingoqa: Visual question answering for autonomous driving. In *European Conference on Computer Vision*, pages 252–269. Springer, 2024. 2
- [35] SungYeon Park, MinJae Lee, JiHyuk Kang, Hahyeon Choi, Yoonah Park, Juhwan Cho, Adam Lee, and DongKyu Kim. Vlaad: Vision and language assistant for autonomous driving. In *Proceedings of the IEEE/CVF Winter Conference on Applications of Computer Vision*, pages 980–987, 2024. 1, 2
- [36] Karl Pertsch, Kyle Stachowicz, Brian Ichter, Danny Driess, Suraj Nair, Quan Vuong, Oier Mees, Chelsea Finn, and Sergey Levine. Fast: Efficient action tokenization for vision-language-action models. *arXiv preprint arXiv:2501.09747*, 2025. 1
- [37] Katrin Renz, Long Chen, Elahe Arani, and Oleg Sinavski. Simlingo: Vision-only closed-loop autonomous driving with language-action alignment. In *Proceedings of the Computer Vision and Pattern Recognition Conference*, pages 11993–12003, 2025. 1, 2, 3, 5, 6, 8
- [38] Hao Shao, Yuxuan Hu, Letian Wang, Guanglu Song, Steven L Waslander, Yu Liu, and Hongsheng Li. Lmdrive: Closed-loop end-to-end driving with large language models. In *Proceedings of the IEEE/CVF Conference on Computer Vision and Pattern Recognition*, pages 15120–15130, 2024. 1
- [39] Zhihong Shao, Peiyi Wang, Qihao Zhu, Runxin Xu, Junxiao Song, Xiao Bi, Haowei Zhang, Mingchuan Zhang, YK Li, Yang Wu, et al. Deepseekmath: Pushing the limits of mathematical reasoning in open language models. *arXiv preprint arXiv:2402.03300*, 2024. 3
- [40] Chonghao Sima, Katrin Renz, Kashyap Chitta, Li Chen, Hanxue Zhang, Chengen Xie, Ping Luo, Andreas Geiger, and Hongyang Li. Drivelm: Driving with graph visual question answering. *arXiv preprint arXiv:2312.14150*, 2023. 2
- [41] Chonghao Sima, Katrin Renz, Kashyap Chitta, Li Chen, Hanxue Zhang, Chengen Xie, Jens Beißwenger, Ping Luo, Andreas Geiger, and Hongyang Li. Drivelm: Driving with graph visual question answering. In *European conference on computer vision*, pages 256–274. Springer, 2024. 1, 5, 6, 2
- [42] Wenchao Sun, Xuewu Lin, Yining Shi, Chuang Zhang, Haoran Wu, and Sifa Zheng. Sparsedrive: End-to-end autonomous driving via sparse scene representation. In *2025 IEEE International Conference on Robotics and Automation (ICRA)*, pages 8795–8801. IEEE, 2025. 1, 2
- [43] Qwen Team et al. Qwen2 technical report. *arXiv preprint arXiv:2407.10671*, 2(3), 2024. 3, 6
- [44] Waywe Research Team et al. Lingo-2: Driving with natural language, 2024. 1
- [45] Kexin Tian, Jingrui Mao, Yunlong Zhang, Jiwan Jiang, Yang Zhou, and Zhengzhong Tu. Nuscenes-spatialqa: A spatial understanding and reasoning benchmark for vision-language models in autonomous driving. *arXiv preprint arXiv:2504.03164*, 2025. 1
- [46] Xiaoyu Tian, Junru Gu, Bailin Li, Yicheng Liu, Yang Wang, Zhiyong Zhao, Kun Zhan, Peng Jia, Xianpeng Lang, and Hang Zhao. Drivevlm: The convergence of autonomous driving and large vision-language models. *arXiv preprint arXiv:2402.12289*, 2024. 1, 2

- [47] Shengbang Tong, David Fan, Jiachen Li, Yunyang Xiong, Xinlei Chen, Koustuv Sinha, Michael Rabbat, Yann LeCun, Saining Xie, and Zhuang Liu. Metamorph: Multimodal understanding and generation via instruction tuning. In *Proceedings of the IEEE/CVF International Conference on Computer Vision*, pages 17001–17012, 2025. 3, 4
- [48] Martin Treiber, Ansgar Hennecke, and Dirk Helbing. Congested traffic states in empirical observations and microscopic simulations. *Physical review E*, 62(2):1805, 2000. 2
- [49] Shihao Wang, Zhiding Yu, Xiaohui Jiang, Shiyi Lan, Min Shi, Nadine Chang, Jan Kautz, Ying Li, and Jose M Alvarez. Omnidrive: A holistic vision-language dataset for autonomous driving with counterfactual reasoning. In *Proceedings of the Computer Vision and Pattern Recognition Conference*, pages 22442–22452, 2025. 1, 2, 3
- [50] Wenhai Wang, Jiangwei Xie, ChuanYang Hu, Haoming Zou, Jianan Fan, Wenwen Tong, Yang Wen, Silei Wu, Hanming Deng, Zhiqi Li, et al. Drivemlm: Aligning multi-modal large language models with behavioral planning states for autonomous driving. *arXiv preprint arXiv:2312.09245*, 2023. 1, 2
- [51] Xinshuo Weng, Boris Ivanovic, Yan Wang, Yue Wang, and Marco Pavone. Para-drive: Parallelized architecture for real-time autonomous driving. In *Proceedings of the IEEE/CVF Conference on Computer Vision and Pattern Recognition*, pages 15449–15458, 2024. 1, 2
- [52] Katharina Winter, Mark Azer, and Fabian B Flohr. Bev-driver: Leveraging bev maps in llms for robust closed-loop driving. *arXiv preprint arXiv:2503.03074*, 2025. 1
- [53] Penghao Wu, Xiaosong Jia, Li Chen, Junchi Yan, Hongyang Li, and Yu Qiao. Trajectory-guided control prediction for end-to-end autonomous driving: A simple yet strong baseline. *Advances in Neural Information Processing Systems*, 35:6119–6132, 2022. 6
- [54] Jinheng Xie, Weijia Mao, Zechen Bai, David Junhao Zhang, Weihao Wang, Kevin Qinghong Lin, Yuchao Gu, Zhijie Chen, Zhenheng Yang, and Mike Zheng Shou. Show-o: One single transformer to unify multimodal understanding and generation. *arXiv preprint arXiv:2408.12528*, 2024. 3, 4
- [55] Zebin Xing, Xingyu Zhang, Yang Hu, Bo Jiang, Tong He, Qian Zhang, Xiaoxiao Long, and Wei Yin. Goalflow: Goal-driven flow matching for multimodal trajectories generation in end-to-end autonomous driving. In *Proceedings of the Computer Vision and Pattern Recognition Conference*, pages 1602–1611, 2025. 1, 2, 5
- [56] Zhenhua Xu, Yujia Zhang, Enze Xie, Zhen Zhao, Yong Guo, Kwan-Yee K Wong, Zhenguo Li, and Hengshuang Zhao. Drivegpt4: Interpretable end-to-end autonomous driving via large language model. *IEEE Robotics and Automation Letters*, 2024. 1, 2
- [57] Zhenjie Yang, Yilin Chai, Xiaosong Jia, Qifeng Li, Yuqian Shao, Xuekai Zhu, Haisheng Su, and Junchi Yan. Drivemoe: Mixture-of-experts for vision-language-action model in end-to-end autonomous driving. *arXiv preprint arXiv:2505.16278*, 2025. 3
- [58] Shuang Zeng, Xinyuan Chang, Mengwei Xie, Xinran Liu, Yifan Bai, Zheng Pan, Mu Xu, and Xing Wei. Futuresight-drive: Thinking visually with spatio-temporal cot for autonomous driving. *arXiv preprint arXiv:2505.17685*, 2025. 1
- [59] Jiang-Tian Zhai, Ze Feng, Jinhao Du, Yongqiang Mao, Jiang-Jiang Liu, Zichang Tan, Yifu Zhang, Xiaoqing Ye, and Jingdong Wang. Rethinking the open-loop evaluation of end-to-end autonomous driving in nuscenes. *arXiv preprint arXiv:2305.10430*, 2023. 6
- [60] Wenzhao Zheng, Weiliang Chen, Yuanhui Huang, Borui Zhang, Yueqi Duan, and Jiwen Lu. Occworld: Learning a 3d occupancy world model for autonomous driving. In *European conference on computer vision*, pages 55–72. Springer, 2024. 1
- [61] Wenzhao Zheng, Ruiqi Song, Xianda Guo, Chenming Zhang, and Long Chen. Genad: Generative end-to-end autonomous driving. In *European Conference on Computer Vision*, pages 87–104. Springer, 2024. 1, 2
- [62] Chunting Zhou, Lili Yu, Arun Babu, Kushal Tirumala, Michihiro Yasunaga, Leonid Shamis, Jacob Kahn, Xuezhe Ma, Luke Zettlemoyer, and Omer Levy. Transfusion: Predict the next token and diffuse images with one multi-modal model. *arXiv preprint arXiv:2408.11039*, 2024. 3, 4
- [63] Xingcheng Zhou, Xuyuan Han, Feng Yang, Yunpu Ma, and Alois C Knoll. Opendrivevla: Towards end-to-end autonomous driving with large vision language action model. *arXiv preprint arXiv:2503.23463*, 2025. 1, 3
- [64] Zewei Zhou, Tianhui Cai, Seth Z. Zhao, Yun Zhang, Zhiyu Huang, Bolei Zhou, and Jiaqi Ma. AutoVLA: A vision-language-action model for end-to-end autonomous driving with adaptive reasoning and reinforcement fine-tuning. In *The Thirty-ninth Annual Conference on Neural Information Processing Systems*, 2025. 1, 2, 3, 6

Unifying Language-Action Understanding and Generation for Autonomous Driving

Supplementary Material

Appendix

A. Action Tokenization

A.1. Log-Coordinate Transformation

We visualize the log-transformed coordinate space to facilitate intuitive comparison. We devise a non-uniform quantization scheme that prioritizes precision near the ego-vehicle by first applying a non-linear transformation to the waypoint coordinates (x, y) along each axis independently.

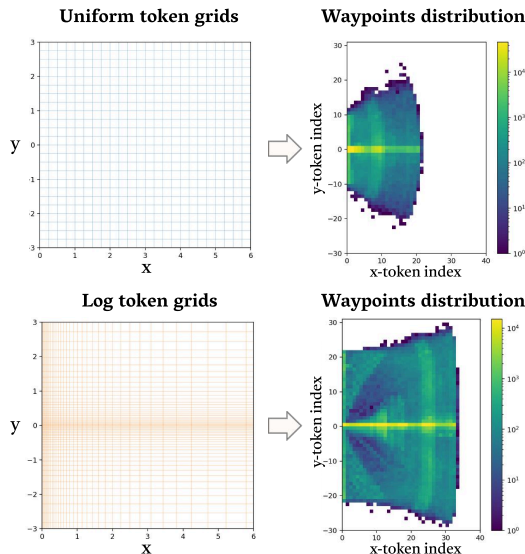


Figure S1. Comparison of uniform and log token grids, with the corresponding waypoint distributions under each grid.

A.2. Number of Action Tokens

We evaluate the effect of the number of action tokens on driving performance on the Bench2Drive [19] benchmark. To this end, we adopt a non-uniform quantization scheme that prioritizes precision near the ego-vehicle by first applying a non-linear transformation to the waypoint coordinates (x, y) along each axis independently. Specifically, each coordinate $z \in \{x, y\}$ is transformed using a signed logarithmic function:

$$z' = \text{sign}(z) \cdot \log(1 + k \cdot |z|). \quad (\text{S1})$$

We then vary the symmetric logarithmic (symlog) scaling factor k from 5.0 to 10.0, which increases the number

of action tokens from 5,656 to 7,245. The parameter k controls the mapping from physical coordinates (both x and y , in meters) to the transformed space, determining the degree of compression prior to binning and, in turn, the effective bin widths in the original coordinate space.

Table S1. Effect of the number of action tokens (controlled by k) in closed-loop evaluation [7].

Method	Driving Score \uparrow	Success Rate (%) \uparrow
$k = 5.0$ (5,656 tokens)	91.01	74.55
$k = 10.0$ (7,245 tokens)	89.85	70.45

A.3. Spatial Soft-Labeling

We evaluate the spread scale in the spatial soft-labeling on driving performance on the Bench2Drive [19] benchmark by varying the spread parameter σ from 1.2 to 3.0. Larger σ yields softer targets by broadening the Gaussian smoothing and distributing probability over a wider neighborhood. Specifically, for a ground-truth token a_{gt} , we construct the target distribution $q(a)$ over all action tokens $a \in \mathcal{C}_{\text{action}}$ as a normalized 2D Gaussian centered at the coordinates of a_{gt} :

$$q(a) = \frac{1}{Z} \exp\left(-\frac{\|\text{pos}(a) - \text{pos}(a_{gt})\|_2^2}{2\sigma^2}\right), \quad (\text{S2})$$

where $\text{pos}(a)$ maps an action token to its 2D coordinates in the spatial grid, $\|\cdot\|_2^2$ denotes the squared Euclidean distance, σ is a hyperparameter controlling the spread of the distribution, and Z is a normalization constant ensuring $\sum_{a \in \mathcal{C}_{\text{action}}} q(a) = 1$.

Table S2. Effect of the spread scale parameter σ in the spatial soft-labeling in closed-loop evaluation [7].

Method	Driving Score \uparrow	Success Rate (%) \uparrow
$\sigma = 1.2$	91.01	74.55
$\sigma = 3.0$	89.73	69.55

B. Dataset

B.1. Action Dreaming

We conduct experiments on the *Action Dreaming* [37] dataset and its offline, nonreactive simulator, which generates alternative ego-vehicle trajectories and assesses their feasibility with respect to collision avoidance and traffic-rule compliance. Ego-trajectory prediction is implemented with a kinematic bicycle model controlled by PID controllers (PDM-lite [41]), driven either by perturbed ground-truth actions or by PID commands computed from predefined path waypoints and target speeds. The dataset provides simulator states and short-horizon forecasts for dynamic objects to enable collision checking. The simulator supports several modes (Objects/Collision, Faster, Slower, Target Speed, Lane Changes, Stop) to induce diverse behaviors and trajectories. We use Success Rate as the metric. Each category has its own definition of success, which we detail in the following:

- **Objects (Collision):** This describes the task of driving towards or crashing into specific objects. The path is evaluated first. If the path of the expert trajectory and the ground truth dreamer trajectory is different (Average Displacement Error $ADE > 1.0$) it is counted as success if the predicted path is closer to the ground truth dreamer path than to the expert path ($ADE_{pred2expert} > ADE_{pred2dreamer}$). If the dreamer path is nearly identical to the expert path ($ADE < 1.0$) the instruction is about correct speed predictions (e.g., if the instruction is “drive towards a dynamic object” it is important to get the speed right and not just the path). The success is then defined as $ADE_{pred2dreamer} < 1.0$ and the average predicted speed is within 30% of the ground truth dreamer speed.
- **Faster (Speed up):** For each predicted speed waypoint, derive target speeds for future timesteps and fit a linear regression to obtain the slope s . Let v denote the current ego speed at the start of the sequence. Success is defined as $s > 0.05 v$.
- **Slower (Slow down):** Same computation as Faster. Success is defined as $s < -0.05 v$.
- **Target Speed:** Since the target speed may not be reached in the prediction horizon of the waypoints, predictions are compared with the ground truth actions instead of directly comparing to the target speed. Two rules define success: First, if the predicted target speed inferred from the last two waypoints is in a 20% range of the instructed target speed. Second, if the predicted target speed inferred from the last two waypoints is in the 20% range of the speed of the last two waypoints of the ground truth speed waypoints. This can be different from the instructed target speed due to limitations in the acceleration rates of the

vehicle.

- **Lane Changes:** Compare the final waypoint of the predicted path with the final waypoints of the ground-truth dreamer path and the ground-truth expert path. Success is defined when the predicted final location is closer to the dreamer’s final location than to the expert’s final location.
- **Stop:** Success is defined when the minimum predicted speed over the sequence is below 0.1 m/s.

B.2. VQA-DriveLM

The VQA data from SimLingo [37] are sourced from the DriveLM-Carla [40] dataset and generated using its data-creation pipeline. Question–answer pairs are extracted from the adopted dataset rather than the original DriveLM release; the training split contains 28M QA pairs over 1M frames in Town 12. Evaluation follows DriveLM keyframe selection to focus on informative frames, and the validation split is balanced across answer types. Labels are heuristically auto-generated, and the dataset includes GPT-4–based paraphrase augmentation (up to 20 variants per QA) to mitigate phrase-level overfitting, with variants sampled at load time.

B.3. Commentary

The commentary labels in SimLingo [37] are automatically generated from a subset of saved simulator state using heuristic, template-based rules. Each label comprises: (1) a route action with justification—default “Follow the route,” replaced only for scenarios requiring lane deviation (e.g., obstacle, encroaching vehicle), with phase-specific templates for before/during/after the deviation; (2) a speed action categorized as remain stopped, stop now, maintain (or maintain reduced) speed, increase speed, or slow down, with a special “Wait for a gap before changing lanes” case when stationary prior to a deviation; and (3) a speed reason derived from IDM [48] features that identify the leading object (vehicle/pedestrian/static control) and its attributes/state, from which concise rationales are composed (e.g., due to pedestrian crossing, behind a red SUV, because the light is red/green). When near a junction, an additional notice summarizes other vehicles’ positions and motions (e.g., junction clear, vehicle moving away, oncoming traffic).

C. Qualitative Results

Figure S2 provides further qualitative results from the closed-loop evaluation, illustrating our model’s performance in a variety of driving scenarios.

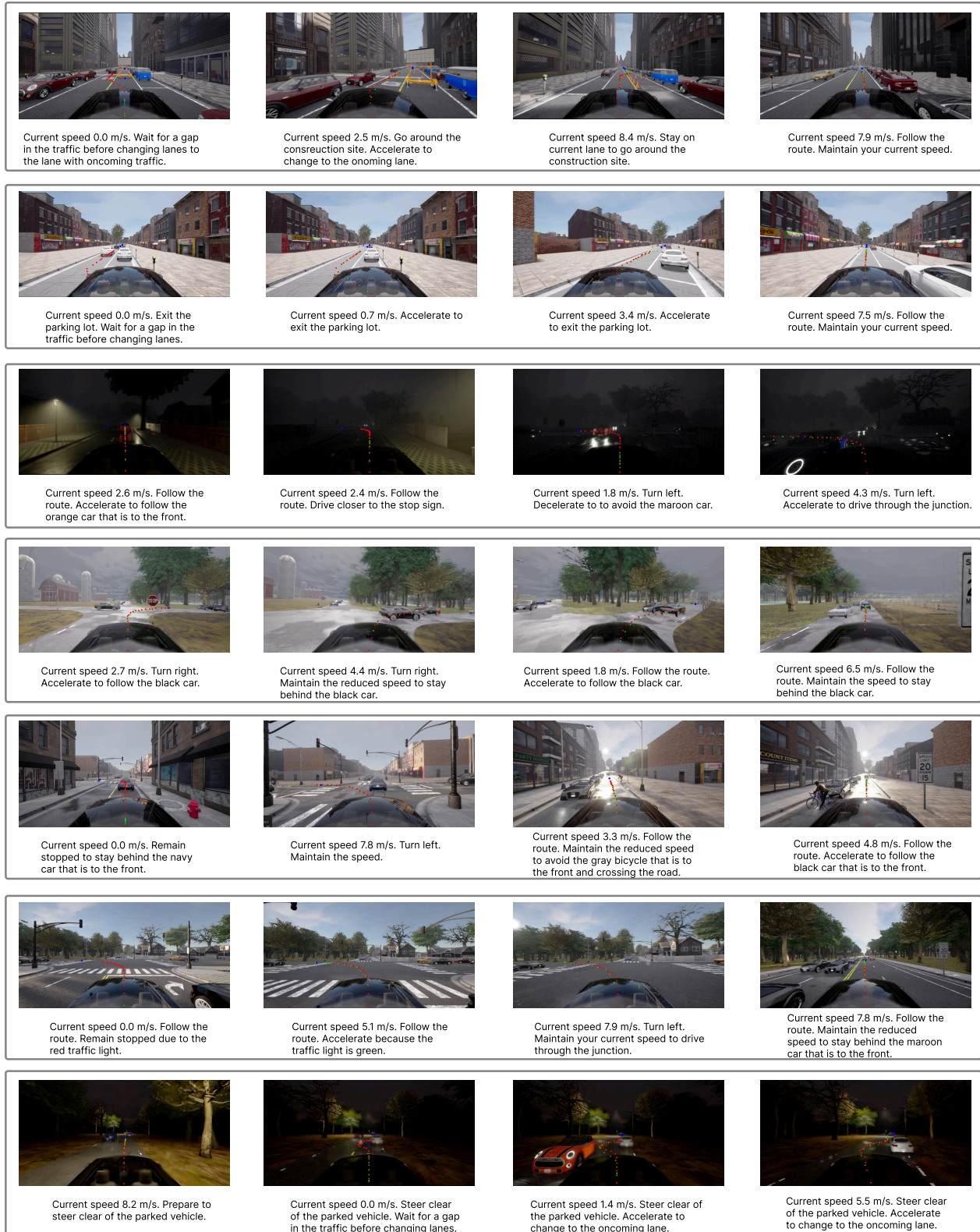


Figure S2. Qualitative results of our proposed model during closed-loop evaluation in the CARLA simulator. The figure showcases representative driving scenarios, such as navigating intersections and avoiding obstacles.